Hindawi Publishing Corporation
ISRN Nanotechnology
Volume 2014, Article ID 634679, 8 pages
http://dx.doi.org/10.1155/2014/634679

Research Article

Heterogeneous Catalysis of C–O Bond Cleavage for Cellulose Deconstruction: A Potential Pathway for Ethanol Production

Kristy Crews,[1,2] Crystal Reeves,[1] Porsha Thomas,[1] Daniel Abugri,[1] Albert Russell,[1] and Michael L. Curry[1,2]

[1] *Department of Chemistry, Tuskegee University, Tuskegee, AL 36088, USA*
[2] *Center for Advanced Materials, Tuskegee University, Tuskegee, AL 36088, USA*

Correspondence should be addressed to Michael L. Curry; currym@mytu.tuskegee.edu

Received 26 September 2013; Accepted 5 December 2013; Published 20 February 2014

Academic Editors: C. Li, R. Redón, and Y.-S. Shon

Due to difficulty deconstructing the linkages between lignin, hemicellulose and cellulose during the conversion of cellulose to sugar, the commercial production of cellulosic ethanol is limited. This can be overcome by using a high surface-area metal catalyst. In this study, high surface-area metal NPs were synthesized using 20 mM of chloroplatinic acid and cobalt chloride prepared in THF with 0.1 mM of generation four poly(amido)amine (PAMAM) terminated dendrimer (G4-NH_2) prepared in methanol and stirred for 2 hours under nitrogen. Subsequently, Pt^{+2} and Co^{+2} ions were reduced to metal zero via introduction of sodium borohydride and centrifuged for complete separation. The resulting product was heated for 2.5 hours at ~200°C. After cooling, 2.0 grams of crushed peanut shells was added to 40 mL of distilled tert-butyl methyl ether along with the separated metal nanocatalyst and refluxed on condenser at 20% for 24 hours. UV-Vis and XRD analyses show the formation of Pt and Co nanoparticles using dendrimer templating methodology. Both TLC and HPLC show that, upon introduction of the metal catalyst into the suspension of "cellulose" in TBME, separation of the cellulose into small molecules is evident. That is, release of sugar molecules via C–O bond cleavage is facilitated by the formed nanocatalysts.

1. Introduction

The anticipated decline in oil production, increased demand on energy usage, and depletion of worldwide petroleum oil reserves have renewed interests in developing alternative energy sources, in particular biofuels. Currently in the United States, 97% of nonrenewable petroleum is used as a source of fuel for vehicles and other gas burning systems [1]. According to the *2012 Consumer Energy Report*, the USA imports about 58% of its petroleum, crude and refined, from the western hemisphere, and consumed 20.7 million barrels of petroleum products in 2007 [2]. One logical solution to this growing energy pandemonium is the development of a sustainable energy alternative, biofuels, that eliminates the United States (and other countries) from the dependency on foreign petroleum imports and the negative impact of anthropogenic CO_2 on the environment. In essence, biofuels use less fossil fuel and, thus, eliminate the fuels formed by natural resources such as anaerobic decomposition of buried dead organisms: coal, petroleum, and natural gases with high percentages of carbon.

Since the 1970s, there have been many types of biomass explored, ranging from agricultural wastes (straw, olive pits, sweet potato roots, and nut shells) to energy crops (*Miscanthus* and *Sorghum*) as a source of producing ethanol [3–7]. Ethanol is an alcohol fuel and can be made from sugars found in corn and barley grains as well as potato skins, rice, sugar cane, sugar beets, and bark. As of date, the United States relies heavily on the production of ethanol from corn, which uses either a wet or dry milling process to convert the corn grains to fuel. It is estimated that ethanol usage in gasoline will double by 2012 (7.5 billion) in comparison to the usage in 2005 [8]. This presents many issues concerning the fuel versus food argument that is raised as ethanolic biofuels are increasingly derived from edible food sources. As a result, sights have turned towards other renewable energy sources, such as cellulose which can be extracted from other sources that do not exist within our food chain. This is considered

an "advanced" biofuel and its production is much more complex than conventional methods (from starches and sugars) [9–11]. Although these methods utilize different feedstocks and processes, conventional ethanol and cellulosic ethanol are the same product. With the cellulosic process, ethanol can be made from trees, grasses, and even crop waste such as peanut shells.

Understanding the usage of nanotechnology as an avenue of producing safe and renewable biofuel will augment the current knowledge base with respect to biofuel production. Based on current methods, essentially this research will further add to the already existing understanding of cellulose separation as well as provide a significant new cost-effective approach to biofuel production. A new methodology whereby metal nanoparticles are used to catalyze C–O bond cleavage, the essential linkage in the lignocellulose network, will be developed in the proposed research. Catalytic methods for the cleavage of C–O sigma bonds are scant because the cleavage of the C–O sigma bond is not a trivial process.

2. Experimental

2.1. Materials. Commercial grade agents purchased from Sigma-Aldrich were used as received. Generation four poly (amido amine) (PAMAM) amine terminated dendrimer (G4-NH_2) as 10% (w/v) methanol solution was purchased from Sigma-Aldrich and used as received. In addition, Pt salts in the form of chloroplatinic acid (H_2PtCl_2) and reducing agent, sodium borohydride ($NaBH_4$), were purchased from Sigma-Aldrich and used as received. Peanut shells were purchased from the local shopping center and used as-received.

2.2. Synthesis of Platinum Nanoparticles. The synthesis of dendrimer-encapsulated Pt NPs was carried out using a similar experimental procedure to that of Street et al. [12]. In this paper, solutions were prepared in the following concentrations: 20 mM of Pt NP, 0.1 mM of G4-NH_2, and 10 mM of $NaBH_4$. Under an atmosphere of N_2, 1 mL of H_2PtCl_6 along with 10 mL of G4-NH_2 was stirred for 2 hours at room temperature. Freshly prepared $NaBH_4$ (10 mL) was added dropwise to the mixture as the reducing agent. Immediately the solution turned dark in color. Subsequently, solutions were then centrifuged, resuspended, and washed with methanol several times. To explore role of the dendrimer encapsulation as a protective layer, parallel solutions of the encapsulated Pt NPs were purged with N_2 and heated for 2.5 hrs at 200°C to remove the protective layer. The resulting products were stored for further chemical reaction and structural analysis.

2.3. Extraction of Sugar Monomers. 2.0 g of peanut shells was obtained and finely ground for 10 minutes using a standard mortar and pestle. Using a round-bottom flask under constant stirring, the ground residue is mixed with 40 mL of distilled tert-butyl-methy-lether, TBME. Subsequently, the dendrimer synthesized NPs were added to the resulting TBME solution and refluxed for a 24-hour period. Given a heterogeneous reaction mixture, the nanoparticles and remaining peanut residue were separated from the sugar solution using standard washing and vacuum filtration procedures. The resulting solutions were then stored for further chemical and structural analysis.

2.4. Characterization of Platinum Nanoparticles

2.4.1. UV-Visible Spectroscopy. Absorbance spectra were collected for the dendrimers and Pt NP salt solutions and for the complexed (Pt-Dens) solutions, before and after chemical reduction. All absorbance measurements were carried out in a 1.0 cm optical path length quartz crystal cuvette and spectra analyses were obtained using a Hewlett-Packard HP 8453 UV-Visible Spectrophotometer. The wavelength range of analysis was 250–800 nm.

2.4.2. X-Ray Diffraction Spectroscopy. Crystal structures of the formed nanoparticles were analyzed using a Rigaku D/MAX 2200 X-ray diffractometer with diffracted beam graphite monochromatic running on Cu Kα radiation. Analysis was performed from 0° to 80° of 2θ angle at a rate of 5 degrees per minute and a sample width of 0.02.

2.4.3. TEM Imaging of Nanoparticles. Electron microscopy images of Pt NPs were carried out using a Zeiss EM10 transmission electron microscope. The fine colloidal suspension was analyzed by depositing 5 μL of Pt NP solution atop a 300 square-mesh, Formvar carbon-coated copper grid (catalog number FCF300-Cu) in ambient conditions and the solvent was allowed to evaporate. The Zeiss EM10 was operated at an acceleration voltage of 60 kV. For each sample, different parts of the grid were used to determine both average shape and size distributions.

2.5. Identification and Characterization of Sugar Extract

2.5.1. Thin Layer Chromatography. Initial identification of the cellulose extraction and deconstruction from peanut shells were analyzed using a standard thin layer chromatography, TLC, system. For the mobile phase, a 3 : 1 ratio of hexanes to ethyl acetate was used. The plate was spotted with the results of refluxes from Pt NP, Co NP, and the standard (peanut shells and distilled tert-butyl methyl ether refluxed for 24 hrs).

2.5.2. High Pressure Liquid Chromatography. Chemical and structural analyses of the deconstructed sugar monomers were carried out using Agilent 1100 series high pressure liquid chromatography (HPLC) system equipped with a diode array detector coupled with a UV-visible (DAD/UV-vis). Samples were analyzed using a SUPELCOGEL C-610H carbohydrate column size 30 cm x 7.8 mm obtained from Sigma Aldrich, Bellefonte, PA, USA. A 0.1% H_3PO_4 was used as the mobile phase with a total run time of 20 mins using an automated injector with injection volume of 20 μL at a flow rate of 1.0 min/mL. The samples for the sugar standards were prepared using 20 mL of HPLC grade water and 0.3 grams of each sugar: β-D-glucose, sucrose, D-(−)-Fructose, and D-(+)-Galactose were all obtained from Sigma Aldrich, MO, USA.

3. Results and Discussion

3.1. UV-Vis Absorption Spectroscopy Analysis. Figure 1 shows UV-Vis spectra of the 0.1 mM dendrimer and 20 mM H_2PtCl_6 salt solutions and of 20 mM of H_2PtCl_6 before and after reduction using $NaBH_4$ in the presence of the dendrimer. It can be observed that, for the aqueous solutions of H_2PtCl_6 and dendrimer, strong absorption bands appear around λ = 465 nm and λ = 280 nm, respectively. However, UV-vis analysis of the H_2PtCl_6 solution in the presence of the dendrimer shows a dramatic change in the resulting spectrum; both absorption bands (λ = 465 nm and λ = 280 nm) are no longer observed indicating that a ligand-to-metal ion transfer between the dendrimer and Pt solutions has occurred. Similar results were reported by Esumi and coworkers after the introduction of H_2PtCl_6 to carboxyl-terminated G4 dendrimers [13]. Furthermore, after reduction, the observance of a dark-brown solution in color and a strong absorption band around λ = 290 nm indicates the formation of zero valent Pt-dendrimer particles.

It has been indicated through the numerous literature reports that the interaction between dendrimers and metals occurs as a result of an ion-pair exchange with the peripheral amine or internal amido groups and depends on the acidity of the and type of peripheral terminal groups placed on modified dendrimers [14]. In this case, we speculate that an ion-pair exchange interaction occurs between the H_2PtCl_6 and the internal amido groups (NH_2) of the dendrimer. This can be explained by the higher acid dissociation constant (ca. 9.4) for external amines in comparison to the internal amido groups and the acidic conditions in which the reaction occurs before reduction (e.g., MeOH and water as solvents). In a slightly acidic medium, the interior amido groups of the dendrimer are protonated resulting in the formation of NH_3^+ and subsequently an electrostatic charge forms between the NH_3^+ and $PtCl_6^{2-}$ moieties creating a network of ion-pair exchange complexes in the interior cavity of the dendrimer. Hence, it is conceivable that, based on this analogy, introduction of the excess $NaBH_4$ will result in the formation of intradendrimer Pt^0 particles; that is, stable dendrimer-encapsulated platinum colloids have been formed.

3.2. XRD and TEM Analysis of Intradendrimer Pt Particles. Previous reports revealed that the mean diameters of dendrimer synthesized Pt nanoparticles are insensitive to the diameter of the free-void-volume space located within the macromolecular interior of the dendrimer. Particles with sizes ranging between 1.4 and 2.5 nm were observed. Figures 2(a) and 2(b) show a representative plan view TEM micrograph and corresponding size-distribution histogram, respectively, of the as-prepared dendrimer-mediated zero valent Pt particles. Analysis of the TEM micrograph in Figure 2(a) clearly reveals that the as-prepared Pt nanoparticles are roughly spherical in shape and uniform in size. It has been speculated that the observance of the larger darker spots is attributed to aggregation of the Pt particles within the dendrimer interior. Esumi and coworkers [13] reported that, at ratios of 40 : 1, [G3-dendrimer]/[Pt^{+2}], respectively, stable particles of Pt could not be achieved and aggregation

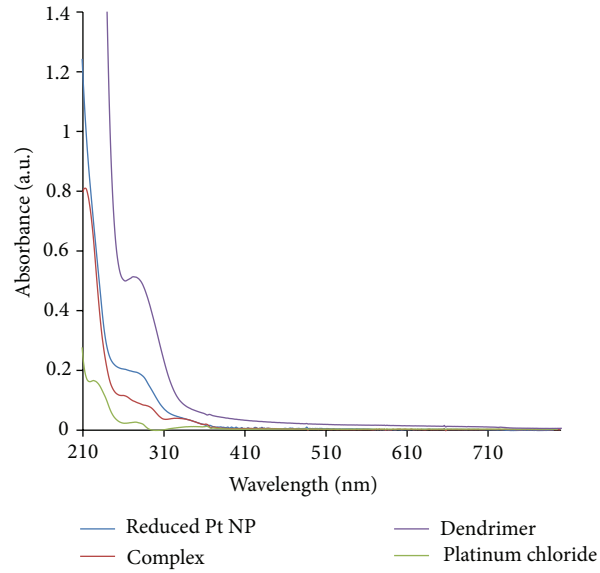

Figure 1: UV-vis spectra of G4-NH_2 and Pt^{+2} interactions before and after reduction with $NaBH_4$.

was observed. In our case, the [G3-dendrimer]/[Pt^{+2}] ratio is 40 : 1; however, given that the diameter of a G4-NH_2 PAMAM dendrimer in solution is on the order of 4.5 nm, it is inconceivable that aggregation of intradendrimer particles will occur on this scale. That being said, the darker regions in this case should be assigned to overlapping of intradendrimer Pt particles as a consequence of the TEM sample preparation method. Similar overlapping of intradendrimer particles was reported by Street and coworkers during the formation of dendrimer-mediated FePt nanoparticles [12].

Figure 2(b) reveals the monodispersity of as-synthesized dendrimer Pt NPs. Excluding the overlapping particle regions, an average diameter of 5.0 nm was measured. This was further confirmed by XRD analysis. Using Debye-Scherrer equation and based on the FWHM of the (111) XRD reflection plane, an estimated average particle size of 4.8 nm was calculated, which is in good agreement with the observed average size using the TEM distribution statistics graph (see Figure 3). Sizes observed here are slightly larger than what is reported in the literature by other studies for Pt using dendrimers as the hosting media for particle formation. A plausible explanation for the increased particle size, in this case, can be reached through examination of the nature of the [dendrimer]/[Pt^{+2}] interaction. Given that the Pt undergoes a slow ligand-exchange reaction involving the tertiary amine groups of the dendrimer, it is possible that the ratio of [dendrimer]/[Pt^{+2}] depends solely on the amount of complexation time allowed before introduction of $NaBH_4$, reducing agent. Hence, higher ratios of [dendrimer]/[Pt^{+2}] should yield slightly larger particles confined within the interior free-void-volume space of the dendrimer structure. Similar results have been observed for formation of Pd particles [15]. Furthermore, observance of the (111) and (200) XRD peaks is indicative of the presence of a chemically disordered face-centered cubic (fcc) structure. That is, monodispersed

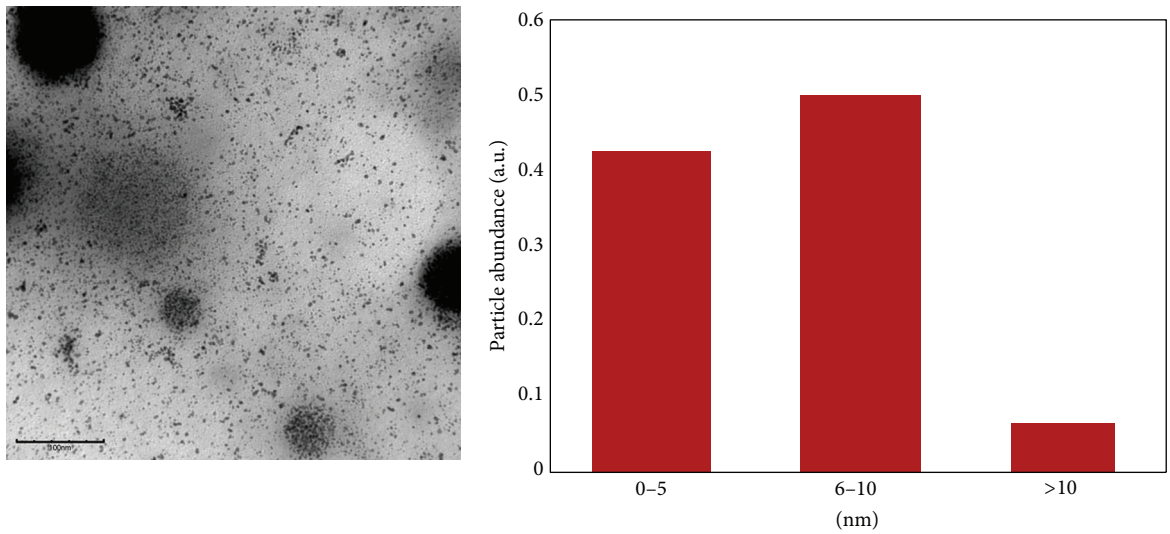

FIGURE 2: TEM analysis (a) and histogram (b) revealing shape and average particle size, respectively, after reduction with $NaBH_4$.

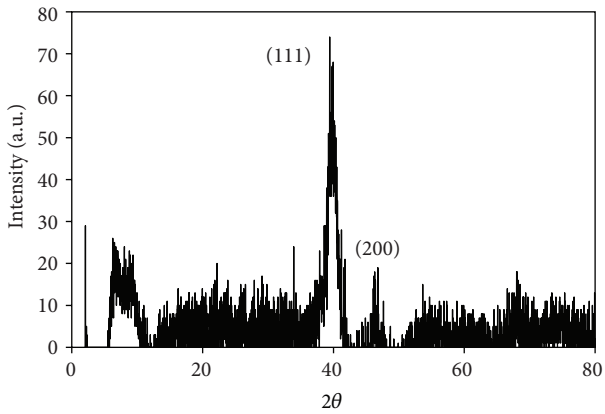

FIGURE 3: XRD analysis of Pt particles after reduction with $NaBH_4$ indicating a face-centered cubic crystal structure.

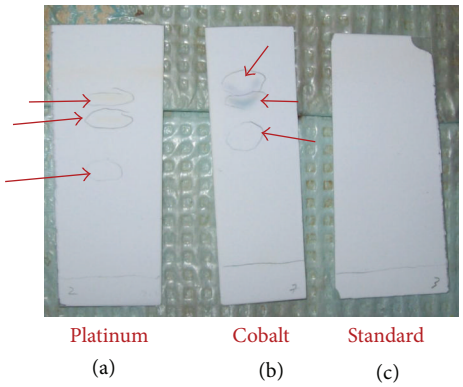

FIGURE 4: TLC analysis of the deconstruction of lignocelluloses upon introduction of nanoparticles ((a) and (b)) and peanut shell standard (c) revealing component separation.

fcc Pt particles with highly controllable sizes (ca. 5.0 nm) have been synthesized.

3.3. HPLC and TLC Analysis of Nanoparticle-Mediated Deconstructed Cellulose. TLC and HPLC analyses indicate that, when peanut shells are treated with platinum nanoparticles without the presence of hydrogen gas, sugars are indeed released as depicted in Scheme 1. That is, lignocellulose can be deconstructed in a one-step process generating fermentable sugars as biofuel precursors.

Figures 4(a)–4(c) show TLC analysis of the sugar solution deconstruct via nanoparticles templating. Clearly the TLC analysis reveals that the components of the peanut shell mixture have undergone separation during the refluxing process. One may speculate that this is simply the different components of the peanut shell solution given its heterogeneous nature; however, the NPs and all other phased chemical species are removed from the resulting sugar solutions before the TLC process is carried out. Moreover, TLC analysis of the peanut shell solution alone shows no separation of the lignocellulose due to chemical interactions occurring with the TBME solvent (see Figure 4(c)). To further confirm the deconstructing nature of the NPs, dendrimer-mediated Co NPs (Figure 5(b)) were also synthesized and carried through the same process as the Pt NPs and very similar TLC results were obtained for both systems.

A more detailed view of the sugar extract can be observed from the HPLC analysis shown in Figures 5(a) and 5(b). HPLC analysis of the sugar extract which reveals a peak with a retention time close to five minutes is present in Figure 5(a). Based on the standard sugar analysis in Figure 5(b), we believe that the peak is consistent with that of glucose. In addition, it is speculated that, given the broad nature of the peak in Figure 5(a) at a retention time around 5 minutes, a mixture of glucose and sucrose is evident; however, further analyses are needed to completely eliminate this notion.

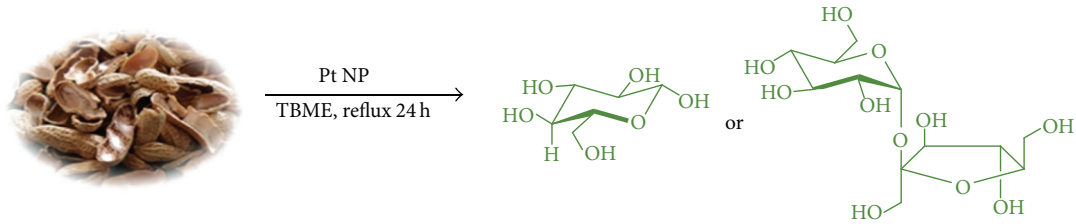

Scheme 1: Pt nanoparticle catalyzed peanut shell decomposition.

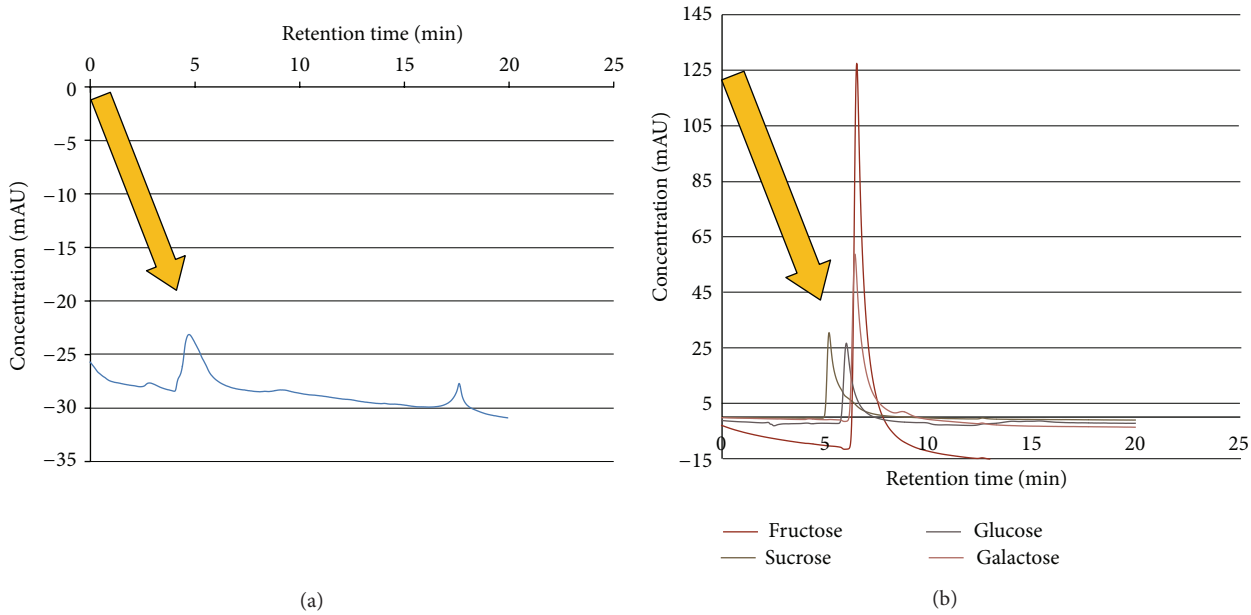

Figure 5: Comparison of (a) sugars obtained from peanut shells to (b) standard glucose, sucrose and fructose.

Another plausible explanation for this slight difference in time scale is the structure of the sugar molecule itself. Depending on whether the sugar monomers are in a beta or alpha structural arrangement, the retention time could be slightly different for either confirmation due to the polarity effect. That is, each structural conformation will exhibit a slightly different interaction with the stationary phase based on the existing arrangements inducing a difference in the migration rate through the column. Similar results were observed by Fukuoka and Dhepe who reported that, under a hydrogen gas atmosphere and in the presence of Pt supported on an aluminum oxide substrate, cellulose was readily decomposed into its sugar units [16]. However, in our case, no hydrogen gas precursor is needed to promote the deconstruction of the cellulose due, as we propose, to the high surface area and extremely reactive nature of the dendrimer-formed NPs.

In this approach, we have designed a one-step process in which the lignocelluloses network can be deconstructed into monomeric sugars without an initial pretreatment step. The process of deconstructing lignocelluloses network normally involves the harsh acidic or basic pretreatment steps to free up cellulose, which is eventually hydrolyzed into sugar monomers [17]. Taking into consideration that lignin is 48–50% β-O-4 linkages (Scheme 2) [18] and that a Ru catalyst system has been shown to depolymerize an analog of lignin [19], a catalyst that is able to do both hydrogen shuttling and C–O insertion should, in principle, be able to depolymerize lignin and break down cellulose into monomers as well. Scheme 2 shows the similarities between lignin and cellulose; both share a motif that may be exploited for dehydrogenation/C–O insertion.

Based on our chemical accounts in this report, it is suggested that the proposed mechanism reported for ruthenium by Nichols et al. (Scheme 3) is an accurate depiction of how platinum particles are able to deconstruct cellulose, as well [19]. In addition, this mechanism can be extrapolated with the conclusion that any metal, with similar capabilities, will follow the same mechanistic pathway, which is further supported by the similar results obtained for the dendrimer-templated cobalt NPs. For instance, as can be seen in the TLC analysis of the reaction mixture where cobalt NPs were refluxed with ground peanut shells (Figure 4(b)), introduction of a less reactive metal in comparison to ruthenium

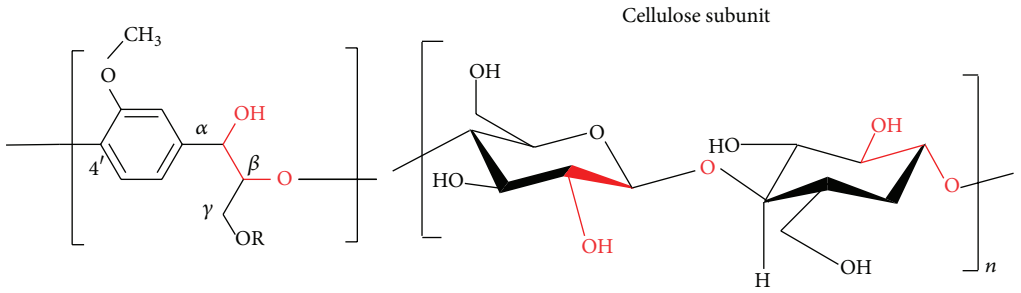

Scheme 2: B-O-4 motif in lignin (left) and ethereal linkage in cellulose.

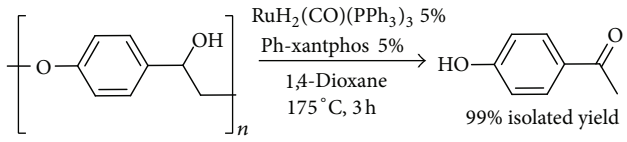

Scheme 3: Lignin analog deconstruction via Ru catalysis

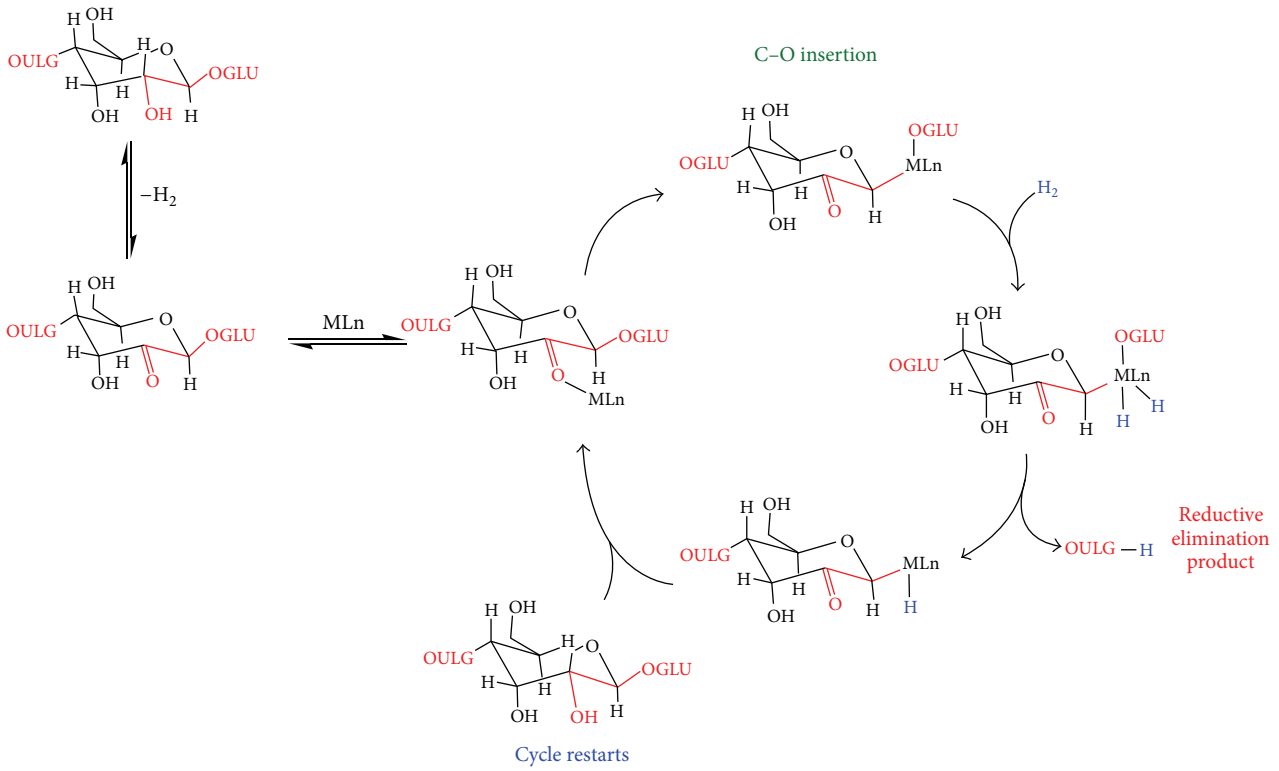

(a)

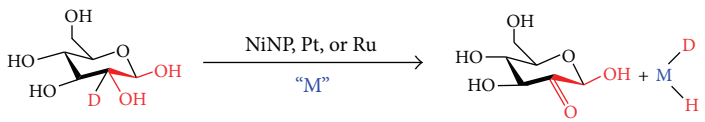

D-[2-2H]glucose

(b)

Scheme 4: Proposed mechanism for cellulose deconstruction via transition metal catalysis.

and platinum exhibits similar separation characteristics of the lignocellulose structure into its components.

This is compelling evidence and, thus, we propose a similar deconstruction pathway which can be rationalized and in which both hydrogen shuttling and C–O insertion are the predominant events that lead to the deconstruction of lignocellulose as well as cellulose. The mechanism whereby lignocellulose is catalytically decomposed using dendrimer-mediated metal NPs is represented in Scheme 4(a). In this proposed mechanism, lignocellulose enters the catalytic cycle in the form of a pyranone, which results from dehydrogenation. Upon entering the catalytic cycle, the glucose subunits (OGLU) are cleaved to release individual glucose units, which can be fermented. The use of a transition metal catalyst, without a pretreatment process, to go from a biomass to glucose makes this a novel process. In order to probe this mechanism, and to determine that hydrogen shuttling is indeed occurring, ongoing experiments with 2H NMR are being explored (see Scheme 4(b)) to investigate glucose with deuterium incorporated in order to determine if deuterium is present on the metal. Indeed, this will confirm the mechanistic approach proposed for the deconstruction of cellulose through a one-step nanocatalyst pathway.

4. Conclusion

In conclusion, we have demonstrated the effectiveness of the dendrimer structure as templates for the formation of nanoparticles that are capable of the deconstruction of lignocelluloses without the need for a pretreatment step. As shown by TEM analysis, the Pt NPs are monodispersed in size and shape and exhibit an overall diameter around 5 nm. XRD reveals a fcc structural arrangement of the as-synthesized Pt NPs as indicated by the observance of the (111) and (200) peaks. HPLC and TLC analyses reveal that the lignocelluloses components are separated upon the introduction of dendrimer-templated nanoparticles. Hence, based on this report, it can be concluded that a new pathway has been reported for the deconstruction of lignocelluloses without the need for the use of harsh acids, that is, a pretreatment step.

Conflict of Interests

The authors declare that there is no conflict of interests regarding the publication of this paper.

Acknowledgments

The authors would like to acknowledge support of this work from the Center for Advanced Materials Science through CREST and ESPCoR awards. Primary support of this work by the Synthesis and Characterization Center and Department of Chemistry at Tuskegee University is gratefully acknowledged.

References

[1] S. C. Davis, "Transportation Energy Data Book 18," Tech. Rep. ORNL-6941, Oak Ridge National Laboratory, Oak Ridge, Tenn, USA, September1998, http://cta.ornl.gov/data/index.shtml.

[2] U.S. Consumer Energy Report, February 2012, http://www.energytrendsinsider.com/research/crude-oil/where-the-us-gets-its-oil-from/.

[3] D. Mohan, C. U. Pittman Jr., and P. H. Steele, "Pyrolysis of wood/biomass for bio-oil: a critical review," *Energy & Fuels*, vol. 20, no. 3, pp. 848–889, 2006.

[4] "Technical, Environmental and Economic Feasibility of Bio-oil in New-Hampshire's North Country," UNH Bio-oil Team Report (Final Report submitted to NH IRC), August 2002 www.unh.edu/p2/biooil/bounhif.pdf.

[5] V. Balan et al., "Process for producing sugars and ethanol using corn stillage," US Patent, 2009.

[6] M. Darapuneni, B. A. Stewart, D. B. Parker, C. A. Robinson, A. J. Megel, and R. E. DeOtte Jr., "Agronomic evaluation of ashes produced from combusting beef cattle manure for an energy source at an ethanol production facility," *Applied Engineering in Agriculture*, vol. 25, no. 6, pp. 895–904, 2009.

[7] USDA Agricultural Baseline Projections to 2015, Paul Westcott, ERS Contact, OCE-2006-1, USDA, Office of the Chief Economist, World Agricultural Outlook Board, February 2006.

[8] "Fuel Ethanol: Background and Public Policy Issues," CRS Report for Congress 2006.

[9] A. Demirbas, "Bioethanol from cellulosic materials: a renewable motor fuel from biomass," *Energy Sources*, vol. 27, no. 4, pp. 327–337, 2005.

[10] J.-C. Frigon and S. R. Guiot, "Biomethane production from starch and lignocellulosic crops: A comparative review," *Biofuels, Bioproducts and Biorefining*, vol. 4, no. 4, pp. 447–458, 2010.

[11] L. S. E. Putri, Nasrulloh, and A. Haris, "Bioethanol production from sweet potato using combination of acid and enzymatic hydrolysis," in *Proceedings of the 2nd International Conference on Mechanical and Aerospace Engineering (ICMAE '11)*, pp. 1767–1772, Trans Tech Publications, Bangkok, Thailand, July 2011.

[12] L. Bai, H. Wan, and S. C. Street, "Preparation of ultrafine FePt nanoparticles by chemical reduction in PAMAM-OH template," *Colloids and Surfaces A*, vol. 349, no. 1–3, pp. 23–28, 2009.

[13] K. Esumi, A. Suzuki, A. Yamahira, and K. Torigoe, "Role of poly (amidoamine) dendrimers for preparing nanoparticles of gold, platinum, and silver," *Langmuir*, vol. 16, no. 6, pp. 2604–2608, 2000.

[14] F. Zeng and S. C. Zimmerman, "Dendrimers in supramolecular chemistry: From molecular recognition to self-assembly," *Chemical Reviews*, vol. 97, no. 5, pp. 1681–1712, 1997.

[15] H. Ye, R. W. J. Scott, and R. M. Crooks, "Synthesis, characterization, and surface immobilization of platinum and palladium nanoparticles encapsulated within amine-terminated poly(amidoamine) dendrimers," *Langmuir*, vol. 20, no. 7, pp. 2915–2920, 2004.

[16] A. Fukuoka and P. L. Dhepe, "Catalytic conversion of cellulose into sugar alcohols," *Angewandte Chemie International Edition*, vol. 45, no. 31, pp. 5161–5163, 2006.

[17] V. B. Agbor, N. Cicek, R. Sparling, A. Berlin, and D. B. Levin, "Biomass pretreatment: Fundamentals toward application," *Biotechnology Advances*, vol. 29, no. 6, pp. 675–685, 2011.

[18] J. Zakzeski, P. C. A. Bruijnincx, A. L. Jongerius, and B. M. Weckhuysen, "The catalytic valorization of lignin for the production of renewable chemicals," *Chemical Reviews*, vol. 110, no. 6, pp. 3552–3599, 2010.

[19] J. M. Nichols, L. M. Bishop, R. G. Bergman, and J. A. Ellman, "Catalytic C-O bond cleavage of 2-aryloxy-1-arylethanols and its application to the depolymerization of lignin-related polymers," *Journal of the American Chemical Society*, vol. 132, no. 36, pp. 12554–12555, 2010.